論文 / 著書情報
Article / Book Information

Title(English)	An Analysis of Multiple Bubble Behaviors in a BWR Suppression Pool
Authors(English)	Motoaki Utamura
Citation(English)	Volume II Thermal-Hydraulics of Nuclear Reactors, Vol. 2, , pp. 1149-1154
Pub. date	1983, 1
Copyright	Copyright (c) 1983 by the American Nuclear Society, La Grange Park, Illinois.

VOLUME II

THERMAL-HYDRAULICS OF NUCLEAR REACTORS

Papers Presented at

The Second International Topical Meeting
on Nuclear Reactor Thermal-Hydraulics
Santa Barbara, California, USA
January 11-14, 1983

Sponsored by the

American Nuclear Society
American Society of Mechanical Engineers
American Institute of Chemical Engineers

Edited by

Mati Merilo
Electric Power Research Institute

Published by the

American Nuclear Society
555 N. Kensington Ave., LaGrange Park, IL 60525, USA

AN ANALYSIS OF MULTIPLE BUBBLE BEHAVIORS IN A BWR SUPPRESSION POOL

by

Motoaki Utamura
Energy Research Laboratory, Hitachi Ltd.
Hitachi, Ibaraki, 316 Japan

ABSTRACT

Dynamics of a multiple bubble system in a BWR suppression pool have been studied considering interactions between bubbles. Based on the potential flow theory, these dynamic interactions have been expressed assuming spherical bubbles. Extension to an arbitrary pool configuration has been made by use of the boundary element method. Numerical results for air bubble oscillation have shown that the interactions cause frequency and magnitude to decrease provided the bubbles oscillate in phase. Experimental verification has also been carried out using simulated air bubbles.

NOMENCLATURE

- f : Frequency, s^{-1}
- F : Load vector, m^2/s^2
- $H_{k\ell}$: Coefficient matrix
- K : Coefficient matrix
- M : Number of boundary divisions
- n : Outward normal vector on the boundary
- N : Number of bubbles
- P : Pressure, Pa
- r_i : Distance from bubble center, m
- r_{ij} : Distance between ith and jth bubbles, m
- R_i : Radius of ith bubble, m
- $\tilde{R}$: Effective radius ($\frac{1}{\tilde{R}} \equiv \frac{1}{R} - \frac{1}{r_e}$), m
- t : Time, s
- $T_{k\ell}$: Coefficient matrix
- u : Fluid velocity, m/s
- W : Fundamental solution to Laplace equation, m^{-1}
- x : Volumetric flow rate ($\equiv R^2 \dot{R}$), m^3/s
- $\tilde{x}$: Vector variable ($\equiv (x_1, x_2, \ldots\ldots x_N)^T$, m^3/s
- α : Angle between vectors n and $r_{i\ell}$, rad.
- δ : Delta function
- $\delta_{k\ell}$: Kronneker delta
- ρ : Density of water, kg/m^3
- ϕ_ℓ : Image potential on ℓ th boundary segment, m^2/s
- ϕ_{ij} : Potential at the center of ith bubble due to image of jth bubble, m^2/s
- ψ_i : Potential field induced by ith bubble, m^2/s
- Γ^1 : Dirichlet boundary (variable given)
- Γ^2 : Neumann boundary (flux given)
- θ : Angle between vectors n and $r_{k\ell}$, rad.

Subscripts

- B : Bubble
- e : Outer range of integration
- i, j : Bubble numbering
- k, ℓ : Element numbering on the pool boundary
- ∞ : Equilibrium

Superscripts

- . : Time derivative
- * : Region ambient to bubble
- T : Transpose

1. INTRODUCTION

Hydrodynamic load may be applied to a BWR containment vessel due to oscillations of air bubbles which are discharged during safety relief valve actuation. Important aspects of this phenomenon include pressure distribution on the pool boundary and the corresponding time history.

Based on the potential flow theory, Lamb solved the dynamics of a single spherical cavity in an infinite pool (1), which was expanded by Antony-Spies to a finite pool with simple geometry using Lagrangian dynamics (2). Giencke also showed that the motion of a single bubble was constrained by the existence of the pool boundary (3).

In application of the previous theories to a multiple bubble system, independent bubble behaviour has been assumed so far. This assumption, however, seems to be valid only if the bubbles are distributed sufficiently far apart. Therefore, the present analysis treats the behaviour of multiple bubble system taking into account dynamic interactions between them. The interaction is formulated in such a way that pool pressure ambient to each bubble is composed of dynamic pressures contributed by the other bubbles. Hence, equations of motion for individual bubbles are expressed in a coupled form and require simultaneous solutions.

The method can be directly extended to a finite pool but in a different way from the previous investigations. For a simple geometry, by using an image source or sink for each bubble, it is possible to convert the original problem into an infinite one where the actual and the image bubbles interact together. Extension to an arbitrary pool configuration is attained by use of the boundary element method. In this formulation, solution form are assumed to be the sum of the fundamental solution to the Laplace equation and an unknown image term.

Numerical results on frequency and magnitude of pressure oscillation are compared with solutions of independent bubble cases. Experimental verification using a simulated air bubble with its submergence changed is also done.

2. ANALYSIS

2.1 Single bubble behaviour in an infinite pool

Assuming incompressible ideal flow and spherical bubble, we have the following conservation equations for fluid :

Momentum :
$$\frac{\partial u}{\partial t} + u\frac{\partial u}{\partial r} = -\frac{1}{\rho}\frac{\partial P}{\partial r} \qquad (1)$$

Mass :
$$r^2 u = R^2 \dot{R} \qquad (2)$$

Integration of eq. (1) in the range of $R \leqq r < \infty$ after substitution of eq. (2) leads to a classical Rayleigh equation :

$$R\ddot{R} + \frac{3}{2}R\dot{R}^2 = \frac{1}{\rho}(P_B - P_\infty) \qquad (3)$$

Dynamic pressure ΔP induced in the pool apart from the center of the bubble can be expressed by

$$\Delta P = \rho\frac{\partial \phi}{\partial t} \qquad (4)$$

where velocity potential ϕ is defined as

$$u = -\nabla\phi \qquad (5)$$

Noting the relation

$$\phi = \frac{X}{r}, \quad X \equiv R^2\dot{R} \qquad (6)$$

from eqs. (2) and (5), we have an alternative form for eq. (4)

$$\Delta P = \frac{\rho}{r}\dot{X} \qquad (7)$$

If we assume each bubble behaves independently, dynamic pressure for a multiple bubble system is given by the method of superposition as follows

$$\Delta P = \rho\sum_{i=1}^{N}\frac{\dot{X}_i}{r_i} \qquad (8)$$

where r_i denotes a distance from the center of the ith bubble to a given location in the pool.

2.2 Multiple bubble behaviours with interactions considered

FIG.1 conceptualizes the interactions between bubbles. The shaded region denotes the range of integration for motion of the ith bubble where the pressure distribution contributed from the other bubbles is assumed to be homogeneous.

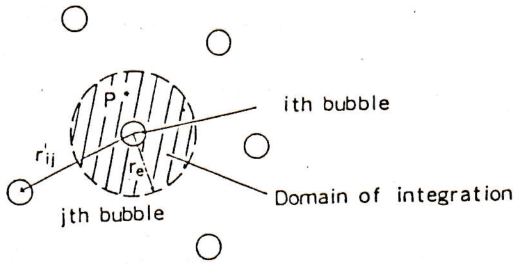

FIG.1 MODELING OF MULTIPLE BUBBLE SYSTEM

With ambient pressure P*, integration of eq. (1) for the ith bubble gives

$$\left(\frac{1}{R_i} - \frac{1}{r_e}\right)\dot{X}_i + \frac{1}{2}\left[\left(\frac{R_i}{r_e}\right)^4 - 1\right]\dot{R}_i^2 = \frac{1}{\rho}(P_{B_i} - P_i^*) \qquad (9)$$

Assuming $(R_i/r_e)^4 \ll 1$ and rewriting pressure in terms of dynamic component ΔP ($\equiv$ P-P_∞), we have an approximation for eq. (9) given by

$$\frac{1}{\tilde{R}_i}\dot{X}_i - \frac{1}{2}\dot{R}_i^2 = \frac{1}{\rho}(\Delta P_{B_i} - \Delta P_i^*) \qquad (10)$$

$$\frac{1}{\tilde{R}_i} \equiv \frac{1}{R_i} - \frac{1}{r_e}$$

Evaluating the ambient pressure ΔP_i^* at the center of the ith bubble, we have

$$\Delta P_i^* = \rho\sum_{j\neq i}^{N}\frac{\dot{X}_j}{r_{ij}} \qquad (11)$$

Substitution of eq. (11) into eq. (10) gives

$$K\dot{\tilde{X}} = F \qquad (12)$$

Where

$$K = \begin{pmatrix} \frac{1}{\tilde{R}_1} & \frac{1}{r_{12}} & \cdots & \frac{1}{r_{1N}} \\ & \frac{1}{\tilde{R}_2} & \cdots & \vdots \\ & \text{Symmetry} & \ddots & \\ & & & \frac{1}{\tilde{R}_N} \end{pmatrix}$$

$$\tilde{X}^T = (X_1, \ldots X_i, \ldots X_N),$$

$$F^T = \left(\frac{X_1^2}{2R_1^4} + \frac{\Delta P_{B_1}}{\rho}, \ldots\ldots, \frac{X_N^2}{2R_N^4} + \frac{\Delta P_{B_N}}{\rho}\right)$$

Off-diagonal terms in matrix K exhibit interactions among bubbles. It is possible to simplify $\tilde{R}_i$ by the following reason. For a situation in which each bubble behaves identically, eq. (12) reduces to a single equation

$$\left(\frac{1}{\tilde{R}_i} + \sum_{j\neq i}^{N}\frac{1}{r_{ij}}\right)\dot{X}_i = \frac{X_i^2}{2R_i^4} + \frac{\Delta P_{B_i}}{\rho} \qquad (13)$$

where $\frac{1}{\tilde{R}_i} + \sum_{j\neq i}^{N}\frac{1}{r_{ij}}$ has a value independent of each bubble. Provided the bubbles are crowded together, $\frac{1}{r_e} \ll \frac{1}{R_i} + \sum_{j\neq i}\frac{1}{r_{ij}}$ holds. Therefore, $\tilde{R}_i$ can be replaced simply by R_i. We assume this approximation in a general case. Substituting the solution of eq. (12) into eq. (8), one obtains dynamic pressure in pool.

2.3 Extension to a finite pool

Solution for velocity potential in a finite pool may be expressed by a combination of fundamental solution and an unknown image term ϕ_i given by

$$\psi = \sum_{i=1}^{N}\psi_i,$$

$$\psi_i = \left(\frac{1}{r_i} + \phi_i\right)X_i \qquad (14)$$

Then, ambient pressure ΔP_i^* corresponding to eq. (11) becomes

$$\Delta P_i^* = \rho \sum_{j\neq i}^{N} \left(\frac{1}{r_{ij}} + \phi_{ij}\right)\dot{X}_j + \rho \phi_{ii}\dot{X}_i \qquad (15)$$

and element K_{ij} of the coefficient matrix K is given by

$$K_{ij} = \frac{1}{r_{ij}} + \phi_{ij} \quad (j\neq i)$$

$$K_{ii} = \frac{1}{R_i} + \phi_{ii} \quad (j=i) \qquad (16)$$

Procedures to obtain the image term are outlined below. Mass conservation gives the following equation

$$\nabla^2 \psi_i + 4\pi X_i \delta(r_i) = 0 \qquad (17)$$

with boundary conditions

$$\frac{\partial \psi_i}{\partial n} = 0 \quad \text{on rigid wall,}$$

$$\psi_i = 0 \quad \text{on free surface.}$$

Inserting eq. (14) into eq. (17), we have an alternative form with variable ϕ_i

$$\nabla^2 \phi_i = 0 \qquad (18)$$

$$\frac{\partial \phi_i}{\partial n} = -\frac{\partial}{\partial n}\left(\frac{1}{r_i}\right) \quad \text{on rigid wall} \quad (\Gamma^2)$$

$$\phi_i = -\frac{1}{r_i} \quad \text{on free surface} \quad (\Gamma^1)$$

Eq. (18) was solved by the boundary element method. Laplace equation (eq. (18)) can be transformed into a boundary integral equation composed of the unknown variable ϕ on the boundary alone.

$$2\pi\phi + \int_\Gamma \phi \frac{\partial W}{\partial n} d\Gamma = \int_\Gamma \frac{\partial \phi}{\partial n} W d\Gamma \qquad (19)$$

Here, W is a fundamental solution to the Laplace equation expressed by

$$W = \frac{1}{r} \qquad (20)$$

FIG.2 illustrates the procedure. Dividing the boundary into M pieces, we have a discretized form of eq. (19)

$$\sum_{\ell=1}^{M} H_{k\ell}\phi_\ell = \sum_{\ell=1}^{M} T_{k\ell}\left(\frac{\partial \phi}{\partial n}\right)_\ell \quad (k=1,M) \qquad (21)$$

$$H_{k\ell} = 2\pi\delta_{k\ell} - \frac{\cos\theta}{r_{k\ell}^2}\Delta\Gamma_\ell$$

$$T_{k\ell} = \frac{\Delta\Gamma_\ell}{r_{k\ell}}$$

with the boundary conditions for the ith bubbles as

$$\phi_\ell = -\frac{1}{r_{i\ell}} \ (\text{on } \Gamma^1), \quad \left(\frac{\partial \phi}{\partial n}\right)_\ell = \frac{\cos\alpha}{r_{i\ell}^2} \ (\text{on } \Gamma^2) \qquad (22)$$

Applying eq. (22) to eq. (21), we can determine ϕ_ℓ on Γ^2 and $\left(\frac{\partial\phi}{\partial n}\right)_\ell$ on Γ^1 respectively for the ith bubble. Repeating this calculation for each bubble, we can obtain N sets of image values and fluxes on the boundary. The velocity potential at the center of the ith bubble defined by the image source of the jth bubble ϕ_{ij} can be evaluated by the following

$$\phi_{ij} = \frac{1}{4\pi}\left\{\int_\Gamma \left(\frac{\partial \phi}{\partial n}\right)_j W_i d\Gamma - \int_\Gamma \phi_j \left(\frac{\partial W}{\partial n}\right)_i d\Gamma\right\} \qquad (23)$$

where $\left(\frac{\partial\phi}{\partial n}\right)_j$ and ϕ_j are given by the previous calculation. Thus, the image term ϕ_{ij} in eq. (16) is obtained. For a simple geometry, the method of image is available. For example, as is shown in FIG. 3, setting up an image source or sink across the boundary to satisfy respective boundary condition only, we can treat the boundary value problem in an infinite domain.

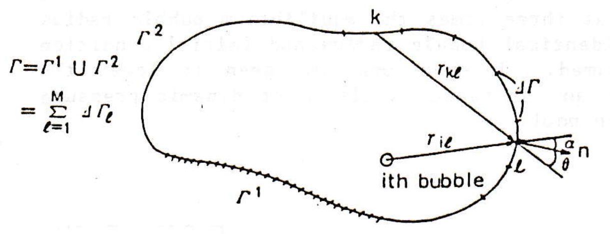

(a) Procedure to obtain ith image on the boundary

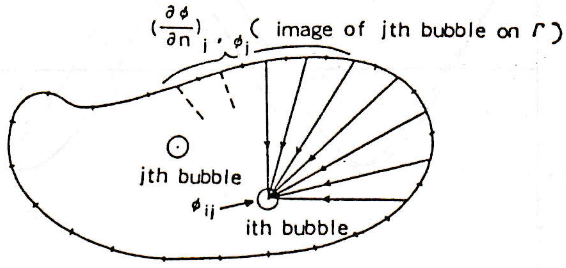

(b) Procedure to obtain potential at ith bubble from the image of the jth bubble

FIG.2 PROCEDURES IN THE BOUNDARY ELEMENT METHOD

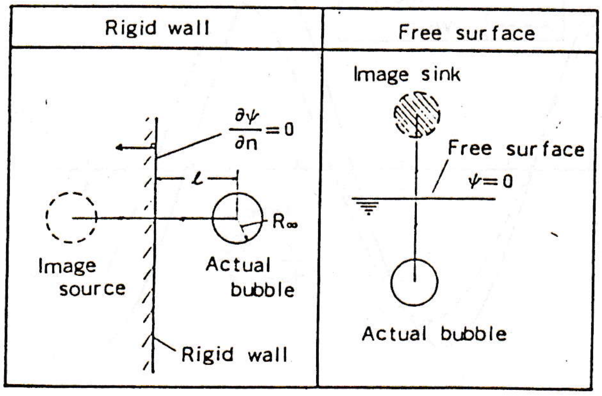

FIG.3 IMAGES FOR SIMPLE GEOMETRY

3. RESULTS AND DISCUSSION

3.1 Effect of bubble interaction

Oscillation by submerged air bubbles was taken as an example to evaluate the effect of interactions between bubbles. Isentropic bubble behaviour was assumed. Behaviours of two bubbles in an infinite pool are shown in FIGs. 4 and 5 with and without interactions between them. Distance between bubbles was set at three times the equilibrium bubble radius value. Identical bubble radius and initial condition were assumed. Interactions are seen to lower the frequency and decrease magnitude of dynamic pressure induced in pool.

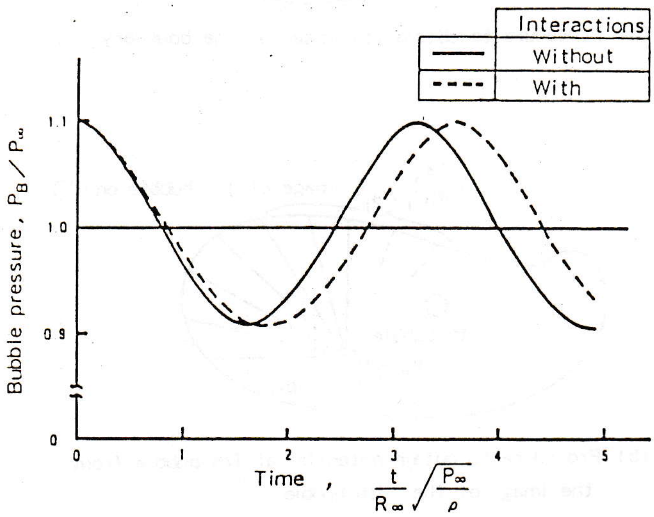

FIG. 4 TIME HISTORY OF BUBBLE PRESSURE

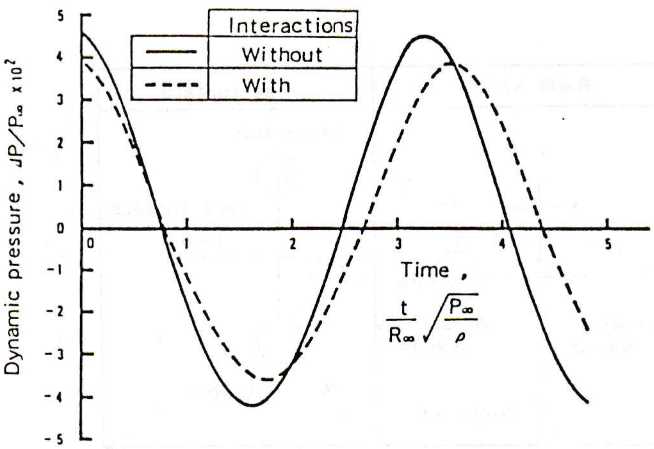

FIG.5 TIME HISTORY OF DYNAMIC PRESSURE IN POOL

FIGs. 6 and 7 show the effect of distance, between two bubbles, with and without interactions for frequency and amplitude of pressure oscillation in the pool. The interactions are significant in the range where the distance between bubbles is kept to less than ten times the equilibrium bubble radius. Hence, one can treat a multiple bubble system without interactions provided they are separated from each other by distances greater than ten times the radius value. One can also conclude that the existence of wall scarcely restricts bubble motion and bubble behavior can be described disregarding the wall effect if distance between wall surface and the center of the bubble exceeds five times the equilibrium bubble radius.

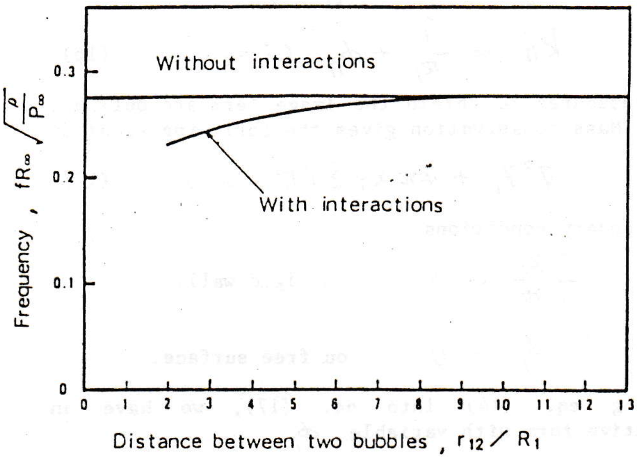

FIG.6 EFFECT OF DISTANCE ON BUBBLE FREQUENCY

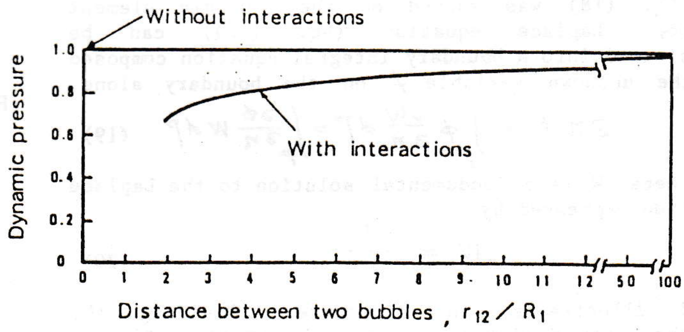

FIG.7 EFFECT OF DISTANCE ON MAGNITUDE OF DYNAMIC PRESSURE

3.2 Effect of the number of bubbles

FIGs. 8 and 9 show the effect of the number of bubbles on frequency and amplitude of dynamic pressure induced in the pool far away from the bubble location. In this analysis, identical bubbles were distributed in a plane in such a manner that distances between adjacent bubbles were kept at three times the equilibrium bubble radius.

Frequency decreases with increasing number of bubbles and approaches an asymptotic value of about seventy percent compared with that of a single bubble. On the other hand, the amplitude of dynamic pressure decreases more rapidly as the number of bubbles increases and reaches about a half that of an independent bubble system if one chooses seven bubble system.

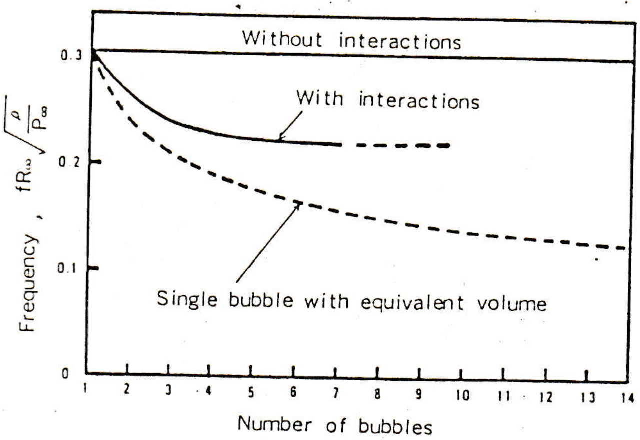

FIG.8 EFFECT OF NUMBER OF BUBBLES ON BUBBLE FREQUENCY

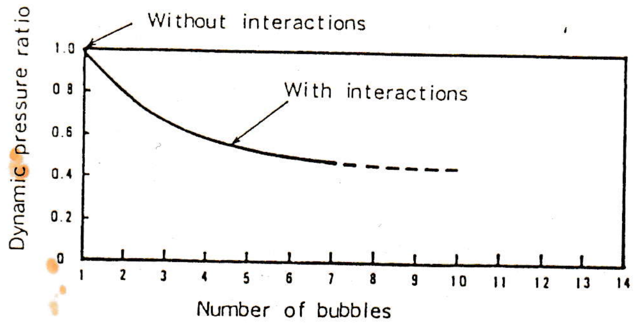

FIG.9 EFFECT OF NUMBER OF BUBBLES ON MAGNITUDE OF DYNAMIC PRESSURE

3.3 Experimental verification

Pressurized air bubbles were discharged through a pipe with its submergence varied as shown in FIG.10. Diameter of the pipe was 53.5mm . Two types of the pipe were used, i.e. straight pipe with open end and a perforated pipe with dead end.

A pressure sensor was located on the tank wall and frequencies of pressure oscillation were measured. In the analysis, the test tank was represented by a rectangular prism whose horizontal cross sectional area was the same as that of the actual tank. Then, boundary conditions for rigid wall and free surface were approximated by the method of imaging. Experiments showed that configuration of the pipe were insensitive to the pressure oscillations. So, a single bubble with equivalent diameter of 58.5cm at atmospheric pressure was assumed in the analysis.

FIG. 11 compares the predictions with experiments in terms of frequency. Frequency increases with decreasing bubble submergence due to reduction of added mass. This tendency was well predicted by the present model mainly due to the existence of the image sink for the free surface boundary conditions. On the other hand, the Minaert formula based on a classical Reyleigh equation was found applicable only if bubble submergence was sufficiently deep.

In the actual suppression pool, guenchers are located apart to each other and the interaction among bubbles are supposed to be small. However, the wall effect can not be ignored because the quenchers are installed in the vicinity of the pool bottom. Hence, the present method can be used to account for the wall effect in the practical application.

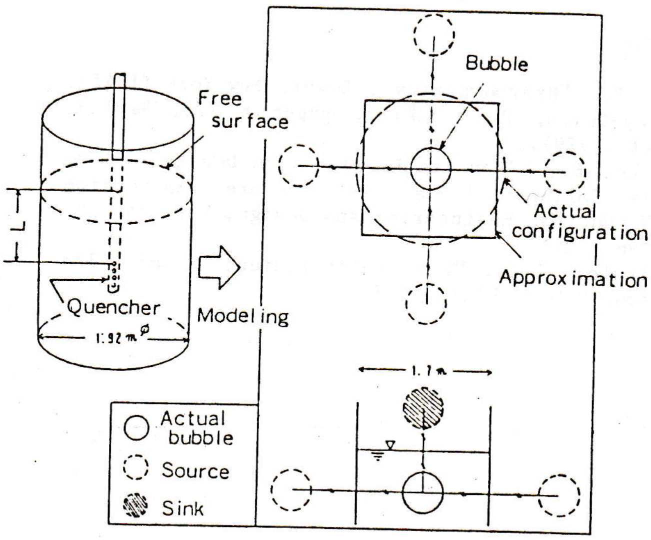

FIG. 10 MODELING OF TEST TANK

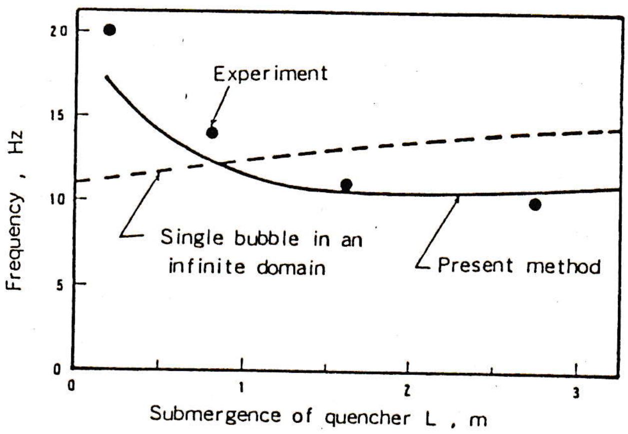

FIG.11 CHANGE OF FREQUENCY WITH BUBBLE SUBMERGENCE VARIED

4. CONCLUSIONS

(1) A numerical method was presented to treat dynamic interactions between multiple bubbles in an infinite pool.
(2) The procedure was given to extend the method to an arbitrary shape of a finite pool.
(3) The interactions were found to restrict bubble motion and reduce amplitude of dynamic pressure in the pool when the bubbles oscillate in phase.
(4) The distances between two bubbles were evaluated to determine when bubble behaviour can be assumed to be independent.
(5) Growth in frequency with less bubble submergence was well predicted by the present model.

ACKNOWLEDGEMENTS

The author would like to express his gratitude to Mr. I. Yokoyama, a technician of Energy Research Laboratory Hitachi Ltd. for his active cooperation in conducting experiment. He is also indebted to Mr. Y. Kato and Dr. K. Taniguchi, manager and general manager respectively of Energy Research Laboratory, Hitachi Ltd. for their encouragements in this work.

REFERENCES

1. Lamb, H., "Hydrodynamics", Dover, New York (1945).
2. Antony-Spies, P., SMIRT-5, paper B 7/3, Berlin, August (1979).
3. Giencke, E., "Pressure Distribution Due to a Steam Bubble Collapse in a BWR Pressure Suppression Pool", Nuclear Engineering and Design, Vol. 65, pp. 175 196(1981).
4 Zienkiewicz, O.C., "The Finite Element Method", 3rd Edition, McGraw Hill (1978).